AD-A049 448 NAVAL RESEARCH LAB WASHINGTON D C F/G 4/1
COMPARISON OF THE 3-5 MICROMETER AND 8-12 MICROMETER REGIONS FO--ETC(U)
DEC 77 A F MILTON, G L HARVEY, A W SCHMIDT

UNCLASSIFIED NRL-8172 SBIE-AD-E000 100 NL

| OF |
AD
A049448

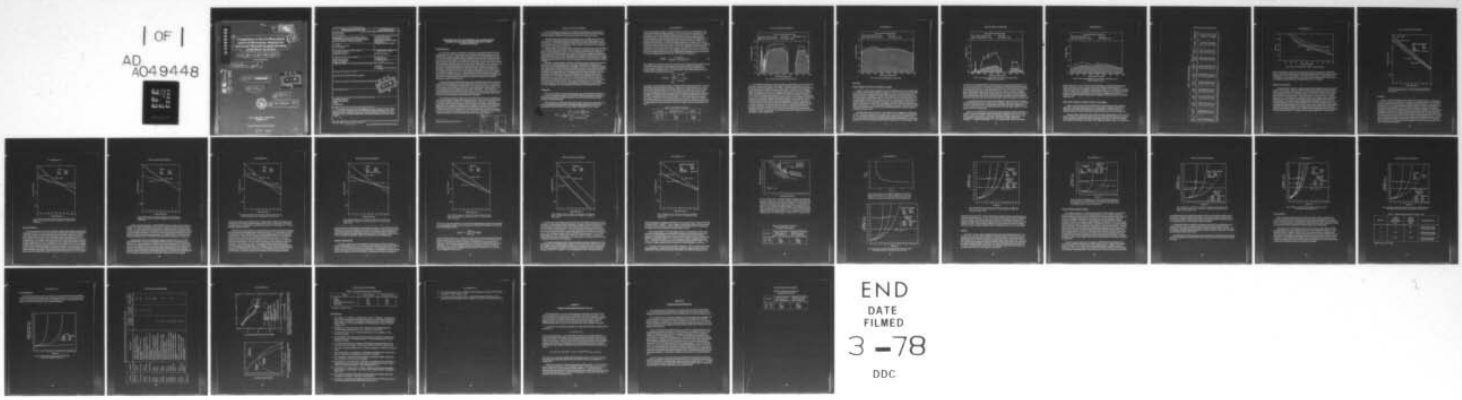

END
DATE
FILMED
3-78
DDC

(6) # Comparison of the 3-5 Micrometer and 8-12 Micrometer Regions for Advanced Thermal Imaging Systems: LOWTRAN Revisited.

(12) 85

(10) A. F. Milton, G. L. Harvey and A. W. Schmidt

Research Department

(9) Interim rept.,

(11) 30 Dec [redacted] 77

(13) 34 p.

(21) SBIE

(19) AD-E000 100

NAVAL RESEARCH LABORATORY
Washington, D.C.

251 950 mt

SECURITY CLASSIFICATION OF THIS PAGE (When Data Entered)

REPORT DOCUMENTATION PAGE		READ INSTRUCTIONS BEFORE COMPLETING FORM
1. REPORT NUMBER NRL Report 8172	2. GOVT ACCESSION NO.	3. RECIPIENT'S CATALOG NUMBER
4. TITLE (and Subtitle) COMPARISON OF THE 3-5 MICROMETER AND 8-12 MICROMETER REGIONS FOR ADVANCED THERMAL IMAGING SYSTEMS: LOWTRAN REVISITED		5. TYPE OF REPORT & PERIOD COVERED Second interim report on a continuing NRL problem. 6. PERFORMING ORG. REPORT NUMBER ETPO Report 41
7. AUTHOR(s) A. F. Milton, G. L. Harvey, and A. W. Schmidt		8. CONTRACT OR GRANT NUMBER(s)
9. PERFORMING ORGANIZATION NAME AND ADDRESS Naval Research Laboratory Washington, DC 20375		10. PROGRAM ELEMENT, PROJECT, TASK AREA & WORK UNIT NUMBERS NRL Problem N01-29
11. CONTROLLING OFFICE NAME AND ADDRESS Department of the Navy Office of Naval Research Arlington, VA 22217		12. REPORT DATE December 30, 1977 13. NUMBER OF PAGES 35
14. MONITORING AGENCY NAME & ADDRESS(if different from Controlling Office)		15. SECURITY CLASS. (of this report) Unclassified 15a. DECLASSIFICATION/DOWNGRADING SCHEDULE

16. DISTRIBUTION STATEMENT (of this Report)

Approved for public release; distribution unlimited.

17. DISTRIBUTION STATEMENT (of the abstract entered in Block 20, if different from Report)

18. SUPPLEMENTARY NOTES

19. KEY WORDS (Continue on reverse side if necessary and identify by block number)

Atmospheric transmission
Electro-optical systems
EOTPO
Imaging systems

20. ABSTRACT (Continue on reverse side if necessary and identify by block number)

Four spectral bands for advanced infrared imaging systems are compared on the basis of calculations of atmospheric transmission, using the LOWTRAN 3B atmospheric transmission model. Slant paths, MTF effects, and Maritime and Rural aerosol models are included in the analysis. The relative advantage of the 3- to 5-micrometer band is shown to be strongly influenced by the choice of aerosol models.

DD FORM 1 JAN 73 1473 EDITION OF 1 NOV 65 IS OBSOLETE
S/N 0102-014-6601

SECURITY CLASSIFICATION OF THIS PAGE (When Data Entered)

COMPARISON OF THE 3-5 MICROMETER AND 8-12 MICROMETER REGIONS FOR ADVANCED THERMAL IMAGING SYSTEMS: LOWTRAN REVISITED

INTRODUCTION

In 1975, Milton, Harvey, Kershenstein, and Mikolosko published a paper on the comparison of the 3- 5- and 8- 12-μm regions for advanced thermal imaging systems, using the LOWTRAN 2 atmospheric transmission computer code to examine the tradeoff as a function of meteorological parameters. Similar comparisons have been made by Barhydt, Brown, and Dorr [2], for the conditions investigated by Taylor and Yates [3], by Schnitzler [4], and by Tam and Corriveau [5]. Thomas W. Tuer [6] has also compared the various methods used by Barhydt, Schnitzler, Milton, and Harvey using LOWTRAN 3A. The evolution of the LOWTRAN atmospheric transmission code is, however, continuing, and the code is upgraded as new experimental data become available and more becomes known about the atmosphere. Because there have been several major changes made in the LOWTRAN code since publication of Ref. 1 in 1975, it was considered worthwhile to make a new comparison using the LOWTRAN 3B code. Comparisons between spectral bands are important at this juncture because the development of new focal plane array detection technologies may negate the conventional wisdom, and different detection technologies need emphasis depending on spectral band preference.

The most important modifications leading to the LOWTRAN 3B code are a reduction of the attenuation coefficient due to the water vapor continuum in the 8- to 14-μm region, the inclusion of an attenuation coefficient due to the water vapor continuum in the 3.5- to 4.2-μm regions, and the addition of three new aerosol models which can be selected at will. The new aerosol models are called the Urban, Rural, and Maritime. They replace the Continental model of the LOWTRAN 2 and 3A code. The most important inputs to the 3B code are still absolute humidity and visibility, although a gradual temperature dependence of the 8- to 14-μm continuum absorption has been introduced.

The comparisons reported in this paper use the LOWTRAN 3B code to consider long-range thermal imaging in humid, fairly clear atmospheres. In all cases the target is assumed to be a small temperature difference ΔT against a uniform background. Atmospheric extinction is used to reduce the apparent contrast at the sensor. Path radiance effects that might change the background irradiance are not considered. Reduction of the modulation transfer function (*MTF*) and image breakup from atmospheric turbulence are also not considered in detail. The comparisons do not include any discussion of smoke penetration, which may be important in battlefield scenarios. Differences in background clutter, which would be important for automatic detection systems, are also not considered.

Manuscript submitted September 23, 1977.

In the comparisons of performance in different spectral bands it is assumed that all detectors operate background limited (BLIP) with the same level of detector technology (the same quantum efficiency and the same immunity to recombination noise).

Considering current technology, this assumption tends to unfairly penalize the 3-to 5-μm band, since high-quantum-efficiency photodiodes are more readily available in the 3- to 5-μm region. Under BLIP operation a *photodiode* can provide an advantage in signal-to-noise ratio of a factor of $\sqrt{2}$ compared to a photoconductor operating in the conventional mode with the same quantum efficiency.

Imaging systems with the same number of detectors, same frame rate, same total field of view, and same instantaneous field of view, but different operating spectral bands are compared in terms of signal-to-noise ratio. In the initial sections of this report comparisons mostly concentrate on horizontal sea level paths. In the initial comparisons the concept of relative signal-to-noise ratio (*SNR*), which ignores the diffraction-limited optical *MTF* advantage of 3- to 5-μm systems is used. *MTF* effects will, however, be considered in the computations presented near the end of the report for slant paths with a maximum altitude of 305 m (1000 ft).

The effect of varying degrees of detector technology (number of detectors) on the preferred choice of operating spectral band is discussed. With advanced imaging systems operating at longer ranges, atmospheric transmittance will become the overriding consideration in the choice of spectral band (along with *MTF* for small or even medium-sized targets). This suggests that the optimum choice of spectral band should be reexamined when considering the use of high-performance focal-plane-array technology which allows the use of thousands of infrared (IR) detectors in an individual system. High humidity tends to penalize the 8- to 12-μm region, whereas poor visibility (scattering from haze) tends to penalize the 3- to 5-μm regions. Thus, it can be expected that under some conditions atmospheric transmittance will favor the 8- to 12-μm region (hazy, dry) and under others, the 3- to 5-μm region (clear, humid). The purpose of this study is to use the updated LOWTRAN 3B atmospheric code [7] and subsequent modifications to examine this tradeoff. The comparisons, of course, depend on the accuracy of the LOWTRAN model.

APPROACH

The approach used was to assume that the target was a small thermal contrast (ΔT = 1°C) on top of a blackbody background near 300 K. Taking the target to be a variation in temperature rather than a variation in emissivity favors the shorter wavelength region; however, it is standard practice.

With the assumptions associated with BLIP operation stated in the introduction, the SNR on a display for a target that subtends a given angular resolution element will be proportional to radiation function $R_{\Delta T}$ as defined by Barhydt et al [2]. That is,

$$R_{\Delta T} = \frac{1}{2\sqrt{2}hc} \frac{\int_0^\infty T_F(\lambda) T_a(\lambda) \frac{\partial W}{\partial T}(\lambda) d\lambda}{\left[\int_0^\infty T_F(\lambda) Q(\lambda) d\lambda\right]^{1/2}}, \quad (1)$$

where C is the velocity of light, h is Planck's constant, $T_F(\lambda)$ is the transmittance of the cooled filter that selects the spectral band, $T_a(\lambda)$ is the atmospheric transmittance at the wavelength λ, W is Planck's spectral emittance function, and $Q(\lambda)$ is Planck's photon spectral distribution. The numerator represents the signal in photons arising from the thermal contrast, whereas the denominator represents the noise from the background. As shown by Kleinhauns [8], the optimum spectral transmission is unity for certain wavelengths and zero elsewhere. An exact optimization depends on the details of $T_a(\lambda)$ and is therefore a function of range to the target. Rather than optimizing for each case comparisons were made of three specific bands, several of which were suggested by Barhydt et al. [2]; namely, the 8.1- to 12.2-μm band, the 3.4- to 5.1-μm band, and the 3.4- to 4.1-μm band. In this report, a relative signal-to-noise ratio $SNR_{rel}^{\Delta\lambda}$ is used; it is unity for the 8.1- to 12.2-μm band at zero range and is reduced by the net atmospheric transmission for the spectral band of interest for target ranges other than zero. With the above assumptions,

$$SNR_{rel}^{\Delta\lambda} = \frac{R_{\Delta T}(\Delta\lambda)}{R_{\Delta T}[8.1 - 12.2, T_a(\lambda) = 1]} . \tag{2}$$

This expression is a function of range R to the target, since T_a is a function of range. The net atmospheric transmission for a given spectral band is simply $SNR_{rel}^{\Delta\lambda}(R)/SNR_{rel}^{\Delta\lambda}(0)$. Another quantity of interest is the relative noise voltage caused by the background, or $(N_b)_{rel}^{1/2}$, again normalized to the 8.1- to 12.2-μm band. For a 300K background, this is a function only of the spectral band chosen:

$$(N_b)_{rel}^{1/2} = \frac{\left[\int_{\Delta\lambda} Q(\lambda)d\lambda\right]^{1/2}}{\left[\int_{8.1}^{12.2} Q(\lambda)d\lambda\right]^{1/2}} . \tag{3}$$

The smaller this is, the harder it will be to obtain background-limited performance. The zero target range comparison is given by Table 1. Clearly, at very short ranges the 8- to 12-μm region has the advantage because of the larger difference in photon flux caused by a given ΔT, and wider spectral bands in the 3- to 5-μm region will be better than narrow ones. This is not necessarily the case for ranges at which atmospheric transmittance can influence $(SNR)_{rel}^{\Delta\lambda}$. An example of the spectral dependence of atmospheric transmittance derived from the LOWTRAN 3B model is shown in Figs. 1-4. The contributions of the various atmospheric constituents to the attenuation are shown in Table 2. Clearly the middle of the 4- to 5-μm region becomes opaque at rather short ranges. With the Rural aerosol model at longer ranges, the region around 4 μm shows up as a super transparent band as shown in Fig. 1.

Table 1—Zero Range Comparison

$\Delta\lambda$ (μm)	$(SNR)_{rel}^{\Delta\lambda}$ for $R = 0$	$(N_b)_{rel}^{1/2}$
8.1 - 12.2	1	1
3.4 - 5.1	0.342	0.154
3.4 - 4.1	0.147	0.056

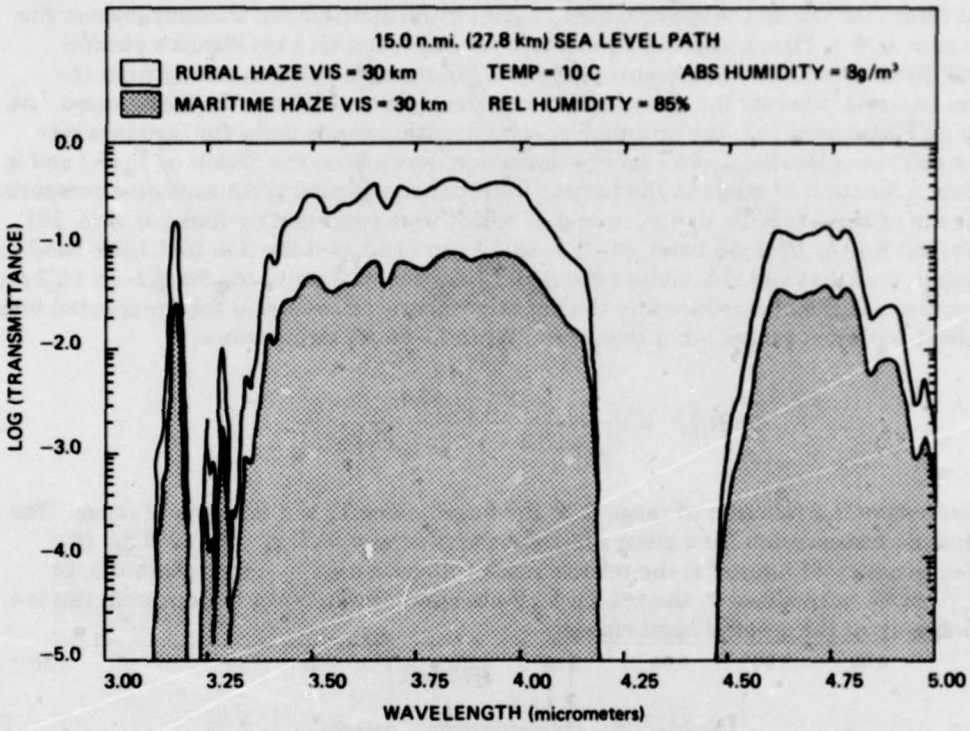

Fig. 1—Plot of typical LOWTRAN 3B code output

The LOWTRAN 3B model computes atmospheric transmittance as a function of wavelength for a range from the sensor to the target. If a standard atmosphere is not used, atmospheric pressure, temperature, ozone density, relative humidity, and sea level meteorological visibility range must be entered into the program. Actually, only two visibility ranges are available: 5 and 23 km. The program interpolates for other values of visibility range. The calculations for sea level conditions were made with a pressure of 100.6×10^9 Pa (1,006 mb), and an ozone density of 6×10^{-5} g/m^3. In fact with the LOWTRAN model only two environmental parameters significantly affect the transmission in the region of interest: meteorological visibility and absolute humidity. Transmission for sea level visibility ranges of 8 km and 23 km and absolute humidities of 14 g/m^{-3} and 19 g/m^{-3} were used to study trends. Results using the LOWTRAN 3B Rural and Maritime aerosol models are compared. For the slant-path calculations, the standard Midlatitude Summer (14 g/m^3) and Tropical models (19 g/m^3) were used; the temperatures and absolute humidities of these two models are the same as the values used for the horizontal path calculations. Figure 5 can be used to convert from the absolute humidities used to relative humidities at various temperatures.

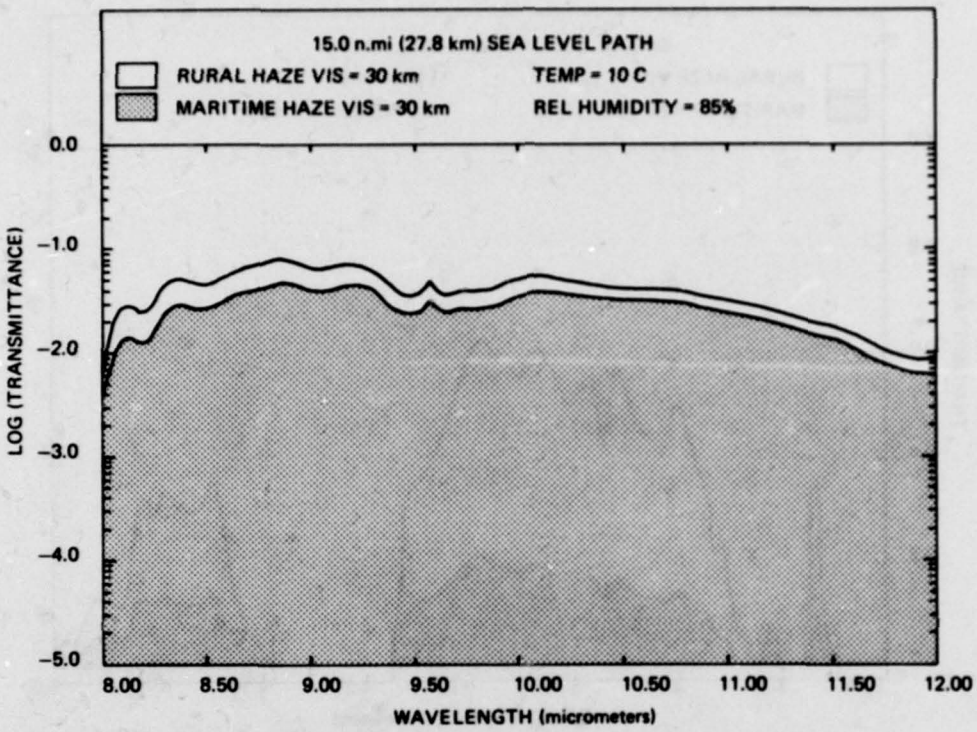

Fig. 2—Plot of typical LOWTRAN 3B code output

RESULTS

Relative Signal-to-Noise Ratios with Respect to Range

Figures 6-13 shows relative signal-to-noise ratio $(SNR)_{rel}^{\Delta\lambda}$ as a function of target range for the variety of atmospheric conditions studied. The curves in Figs. 6-13 are not straight lines when plotted on semilog paper because different parts of the spectral bands have different extinction coefficients. For most of the calculations sea level transmission paths were considered, although targets might well be over the horizon at the longer ranges. In comparing signal-to-noise ratio as a function of range, we assumed that the target subtends the same angular width at the imager for all ranges. This underestimates the decrease in signal-to-noise ratio at the display with increasing range which would be experienced with a target of constant size. A more sophisticated performance analysis would include the effect of diminishing target angular subtense with increasing target range by using the methods developed by Schnitzler [4].

Several different bands in the 8- to 14-μm region have been suggested by various proponents. Four were examined: 8.06-12.2 μm, 8.47-11.11 μm, 8.7-9.76 μm, and 8.06-8.93 μm. A comparison was made for a slant path and the meteorological conditions shown on Fig. 6. As might be expected, the widest bands resulted in better SNR_{rel} at short range, and the 8.47- to 11.11-μm band resulted in the best performance at very long range. Since

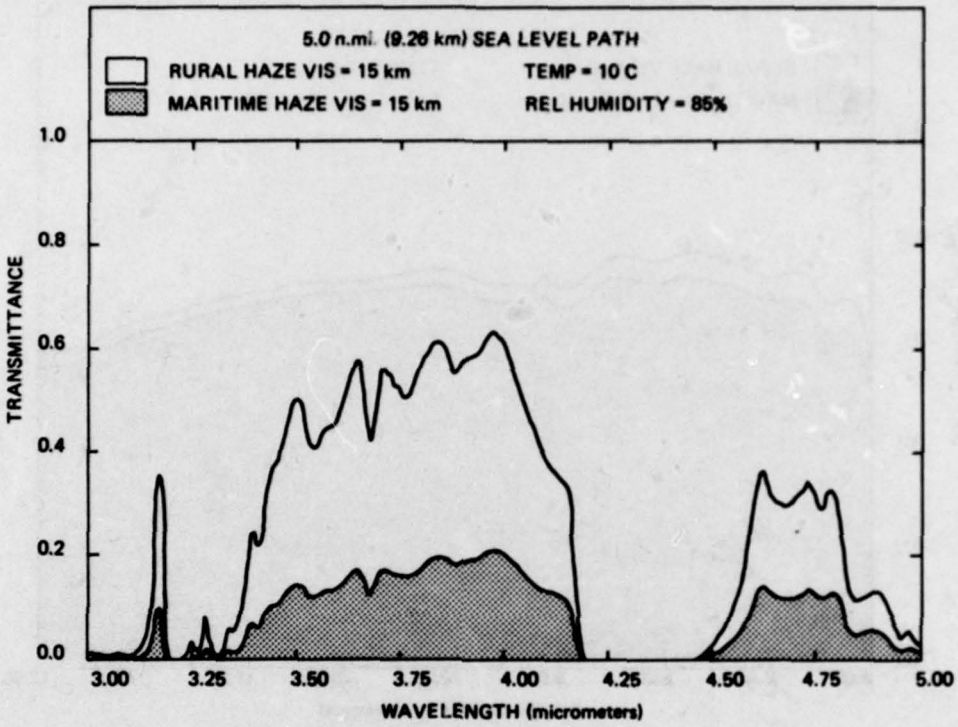

Fig. 3—Plot of typical LOWTRAN 3B code output. Note effect of lower visibility compared to Fig. 1.

in all cases there was little difference between the 8.06- to 12.2-μm band and the 8.47- to 11.11-μm band, the 8.06- 12.2-μm band was retained as the reference band because it was used in the earlier report [1]. Selecting a narrower band can at best only improve $(SNR)_{rel}$ by reducing $(N_b)_{rel}^{1/2}$, which is very nearly proportional to $(\Delta\lambda)^{1/2}$ in the 8- to 12-μm region. Selecting the narrower band in the 8- to 12-μm region will not have a dramatic effect on the signal-to-noise ratio as conventionally defined. However, the use of only the most transparent part of the window may help to avoid observation of spurious thermal fluctuations associated with the turbulent atmosphere, which would appear as pattern noise.

An examination of Figs. 6-13 shows that at ranges less than 8 km the 8.1- to 12.2-μm band is usually superior from the point of view of $(SNR)_{rel}$, whereas at ranges of 20 km and more this is often not the case. At long ranges under fairly clear, humid conditions the 3.4- to 4.1-μm band seems to be the best of all, but by not more than a factor of two compared to the 3.4- to 5.1-μm band.

Figure 7 shows $(SNR)_{rel}^{\Delta\lambda}$ for a sea level path with midlatitude summer conditions, i.e., visibility = 23 km, air temperature 20.9°C and absolute humidity 14 g/m^3 (R.H. = 79%), using the Rural aerosol model. Under these conditions $(SNR)_{rel}^{\Delta\lambda}$ is larger for the 3- to 5-μm bands for ranges beyond about 12 km. We define the range beyond which $(SNR)_{rel}^{3.4\text{-}4.1}$ is larger than $(SNR)_{rel}^{8.1\text{-}12.2}$ as the crossover range. Beyond that range a

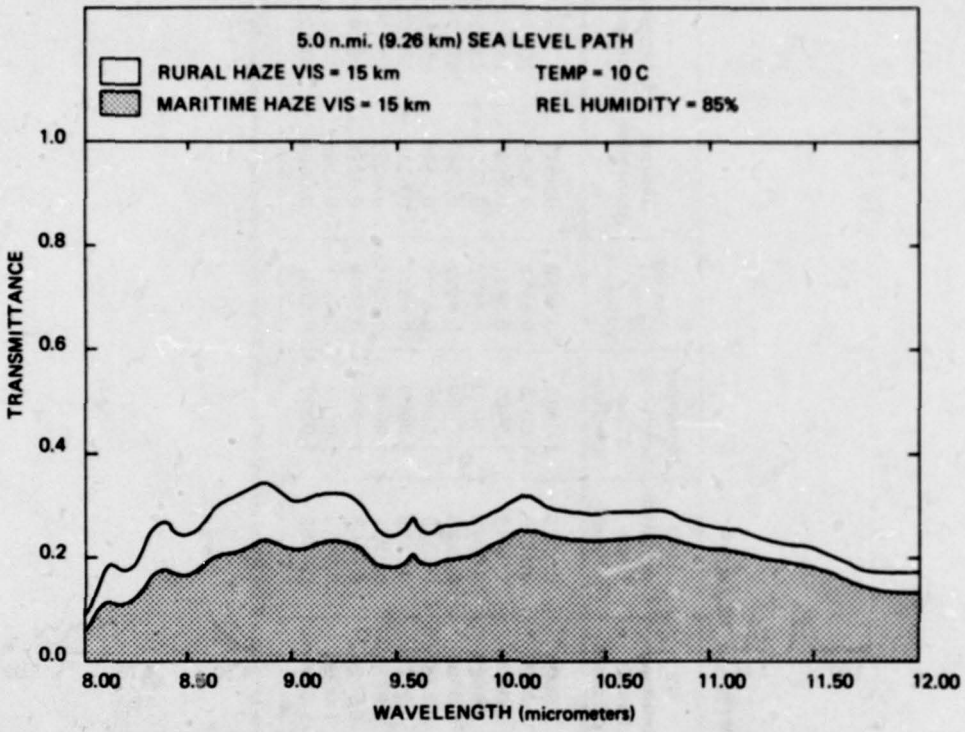

Fig. 4—Plot of typical LOWTRAN 3B code output. Note effect of lower visibility compared to Fig. 2.

system using the 3.4- to 4.1-μm band could be expected to provide higher signal-to-noise ratio for a given ΔT contrast. Figures 8 and 9 show that this crossover range is not appreciably influenced by changing the temperature to 26.9°C or by changing the visibility to 8 km. Indeed, from our experience with LOWTRAN 3B using the Rural aerosol model it is safe to conclude that transmission in the IR bands of interest here is not greatly influenced by small temperature variations or by changes in visibility range down to visibility ranges of 5 km.

Water Vapor Continuum Absorption in the 3- to 5-μm Region

There is concern that the present LOWTRAN 3B model does not predict sufficient water vapor continuum absorption in the 3- to 5-μm region. Appendix A describes the algorithm used to predict this contribution in LOWTRAN 3B. LOWTRAN 3B uses continuum absorption values derived for the data of Burch, Grynak, and Pembroke [9].

Guttman, Horton, and Hanley [10] at NRL have made measurements in the 3- to 5-μm band in an attempt to separate the extinction due to water vapor from that due to aerosols. From preliminary analysis of their data, it appears that the extinction coefficient derived from the NRL data will be up to a factor of two higher than Burch's values. To examine the

Table 2—LOWTRAN 3B Data*

Frequency cm^{-1}	Wavelength (μm)	Total Transmittance	H_2O Transmittance	CO_2+ Transmittance	Ozone Transmittance	N2 Continuum Transmittance	H_2O Continuum Transmittance	Molecular Scattering Transmittance	Aerosol Transmittance	Aerosol Absorption	Integrated Absorption
1820	12.1951	0.0132	0.7669	0.9829	1.0000	1.0000	0.0202	1.0000	0.8699	0.0577	9.87
1920	10.8696	0.0608	0.8441	0.9855	1.0000	1.0000	0.0852	1.0000	0.8581	0.0654	105.94
1020	9.8039	0.0866	0.7919	0.9884	0.8005	1.0000	0.1642	1.0000	0.8421	0.0840	197.44
1120	8.9286	0.1264	0.7093	0.9981	0.9871	1.0000	0.2213	1.0000	0.8172	0.1123	286.56
1220	8.1967	0.0546	0.2661	0.9063	1.0000	1.0000	0.2536	1.0000	0.8921	0.0843	377.02
2440	4.0984	0.3116	0.9927	0.9533	1.0000	0.5382	0.7369	1.0000	0.8304	0.0548	6.88
2540	3.9370	0.5330	0.9542	0.8973	1.0000	0.9177	0.8196	1.0000	0.8276	0.0549	58.35
2640	3.7879	0.4430	0.6625	0.9933	1.0000	0.9893	0.8254	1.0000	0.8245	0.0552	108.70
2740	3.6496	0.4329	0.7020	0.9935	1.0000	0.9994	0.7566	1.0000	0.8208	0.0578	169.49
2840	3.5211	0.2797	0.6120	0.9812	1.0000	1.0000	0.6813	1.0000	0.8171	0.0598	239.11
2940	3.4014	0.1038	0.2995	0.7279	1.0000	1.0000	0.5852	1.0000	0.8135	0.0664	308.29

*The contributions of various atmospheric constituents to the attenuation using the LOWTRAN 3B Rural aerosol model with 23-km meteorological visual range, absolute humidity of 14 g/m^3, air temperature of 20.9°C, and target range of 10 km.

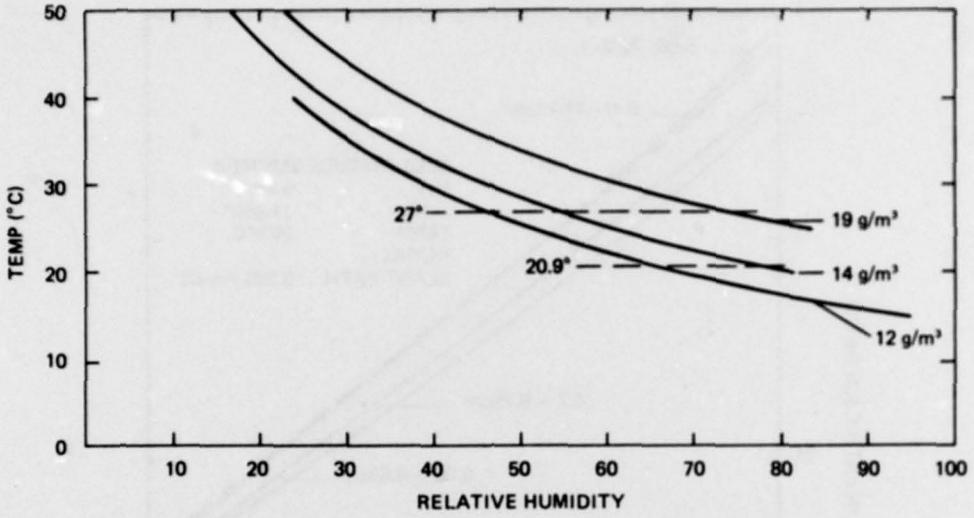

Fig. 5—Chart for converting from relative to absolute humidity

effect of changing the water vapor continuum absorption in this region, the calculations shown in Fig. 7 were repeated with the extinction coefficient due to water vapor continuum doubled for the 3.5- to 4.2-μm region. The results, shown in Fig. 10, show that the crossover ranges are not increased by more than 2 km so that a doubling of this contribution to the extinction coefficient should not significantly alter our conclusions.

Maritime Aerosol Model

A change from the rural to the maritime aerosol model drastically reduces transmission in the 3- to 5-μm region. Figure 11 shows that this change increases the crossover range to 18-20 km for conditions with a humidity of 14 g/m^3 and sea level visibility range of 23 km. Under midlatitude summer conditions this effect is even more noticeable as the visibility range becomes shorter than 23 km. Figure 12 predicts no crossover at all for a visibility range of 8 km. It can therefore be concluded that unless the visibility range is significantly longer than 23 km, conversion to the Maritime aerosol model significantly increases the crossover range. The relation between visibility range (transmission around 0.5 μm) and extinction coefficient due to aerosol scattering in the 3- to 5-μm micrometer region is thus very different for the Maritime aerosol model. This conclusion is also valid for slant paths as modeled by LOWTRAN 3B (Fig. 13). Indeed, in general, the $(SNR)_{rel}^{\Delta\lambda}$ curves for slant paths with a maximum altitude of 305 m (1000 ft) do not differ appreciably from those for sea level horizontal paths. The Maritime model severely penalizes the 3- to 5-μm region.

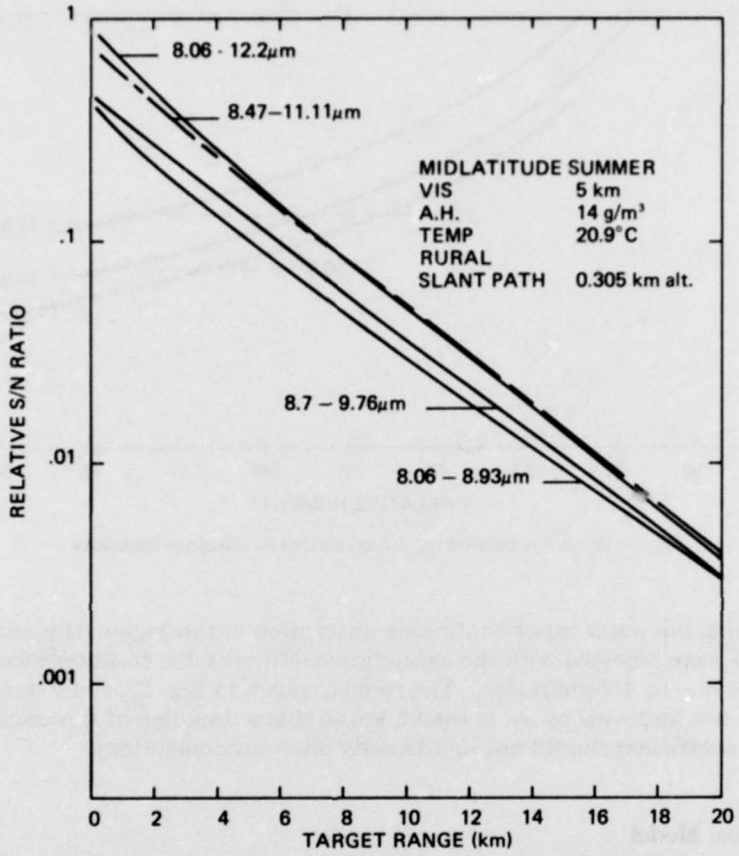

Fig. 6—Relative S/N ratio as a function of range, showing effect of spectral bandwidth in the 8- to 12-μm region. The Rural aerosol model is used.

Humidity

Even with the new LOWTRAN code the effect of absolute humidity on transmission in the 8- to 12-μm region is still strong. Humidity is less influential in the 3- to 5-μm region so that the crossover range decreases as the absolute humidity increases. This leads to an advantage for 3- to 5-μm systems under tropical conditions. Crossover range is plotted as a function of absolute humidity in Fig. 14 for various visibility conditions. Our analysis shows that the curves do not change very much as a function of visibility (>5 km) with the Rural aerosol model; however, Fig. 14 shows that it does shift to shorter ranges and higher humidities as a function of decreasing visibility range if the Maritime aerosol model is used. The curves show that with the Rural aerosol model for target ranges larger than 17 km there can be a significant advantage for 3- to 5 μm systems with humidities above about 12 g/m^3 and for the Maritime aerosol model (visibility of 23 km) above about 14 g/m^3. This conclusion stems from the relatively superior transmission of the band near 4 μm under conditions of high absolute humidity.

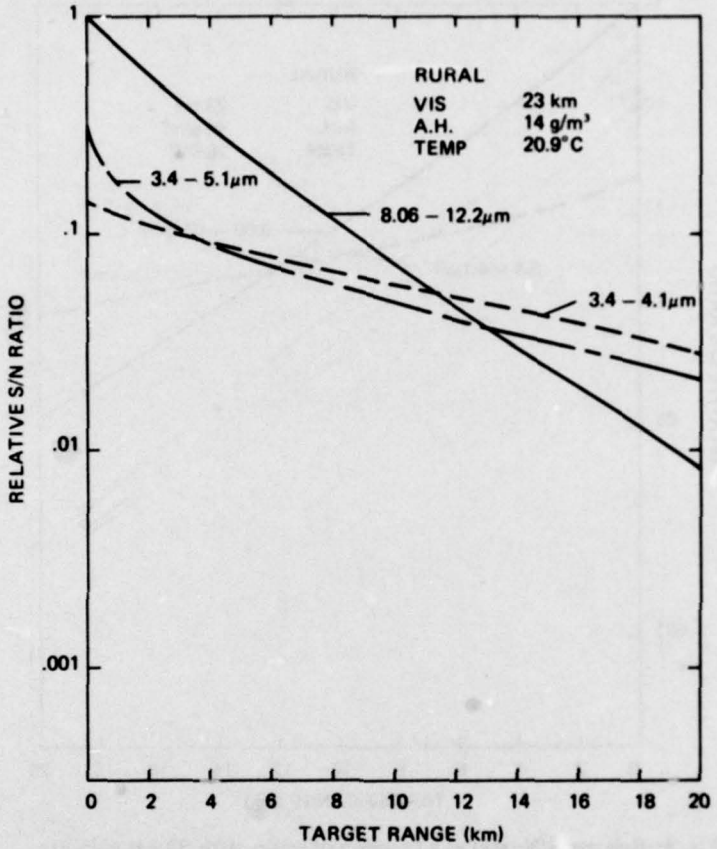

Fig. 7—Relative S/N ratio as a function of range, with 23-km visibility, humidity of 14 g/m^3, and 20.9°C background. The Rural aerosol model is used.

System Performance

The crossover range curves in Fig. 14 delineate ranges of high humidity and long range to the target at which 3- to 5-μm imaging systems should provide relatively larger signal-to-noise ratios. However, the region may or may not be important, depending on whether various imaging tasks of interest can be performed at all at those ranges with available 3-5 μm systems. For example, a relative advantage at target ranges greater than 15 km is worthless if the 3-5 μm imaging system does not provide a high enough signal-to-noise ratio for target ranges beyond 10 km. As emphasized in Ref. 1, designers of present IR imaging systems (≈200 detectors) correctly prefer the 8- to 12-μm band, since a 3- to 5-μm imager with 200 detectors providing imagery with resolution similar to TV would not be sensitive enough to perform most imaging tasks at ranges long enough to obtain the relative atmospheric transmission advantage. This preference remains valid with the LOWTRAN 3B code since most of the changes incorporated in the 3B code work against the 3- to 5-μm region.

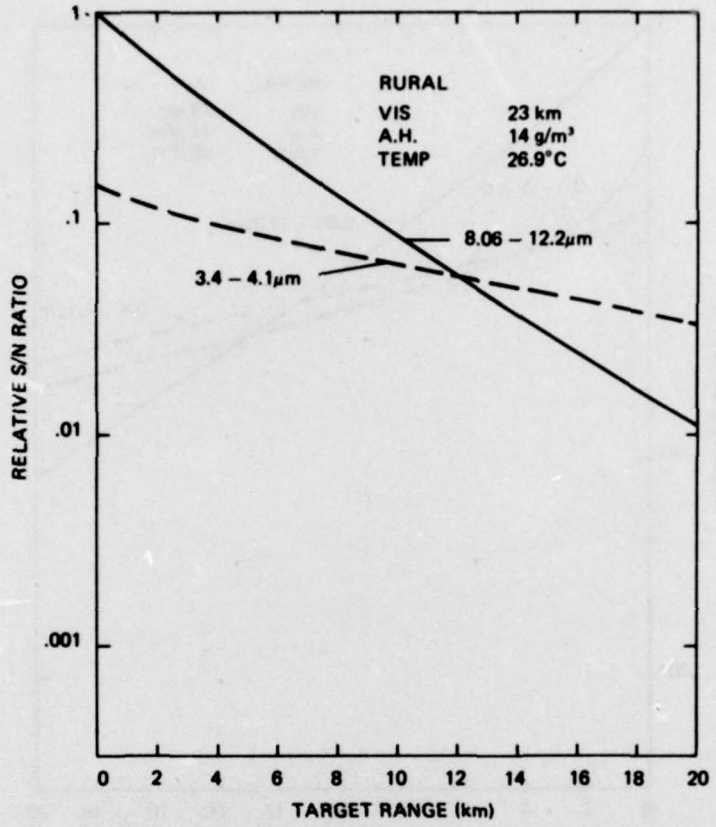

Fig. 8—Relative S/N ratio as a function of range, with 23-km visibility, humidity of 14 g/m^3, and 26.9°C background. The Rural aerosol model is used.

Advanced technology systems (10,000-20,000 IR detectors) could, however, take advantage of the superior transmission near 4 μm that is evident in relatively clear but humid weather. A complete quantitative characterization of this phenomena would require selection of a task and a target, as well as derivation of a minimum resolvable temperature (MRT) curve for an advanced system to use with our curves for atmospheric transmission to gain an estimate of expected maximum operating ranges. To simplify matters, we will make some fairly gross approximations. Their relevance to real situations is discussed in Appendix B.

We assume that a present-technology BLIP imager operating in the 8.1- to 12.2-μm band with 200 detectors can provide adequate imagery down to net atmospheric transmission of 0.1. This corresponds, for example, to a ΔT at the target of 1.0°C and an MRT of 0.1°C at the angular resolution of interest. Since under BLIP conditions, using the same field of view, the signal-to-noise ratio is proportional to the square root of the number of detectors, a future advanced-technology system with 20,000 BLIP detectors operating in the 8-12 μm region would be able to operate effectively down to an atmospheric transmission of 0.01 for the same angular resolution in target space. Equivalent 3- to 5-μm imagers

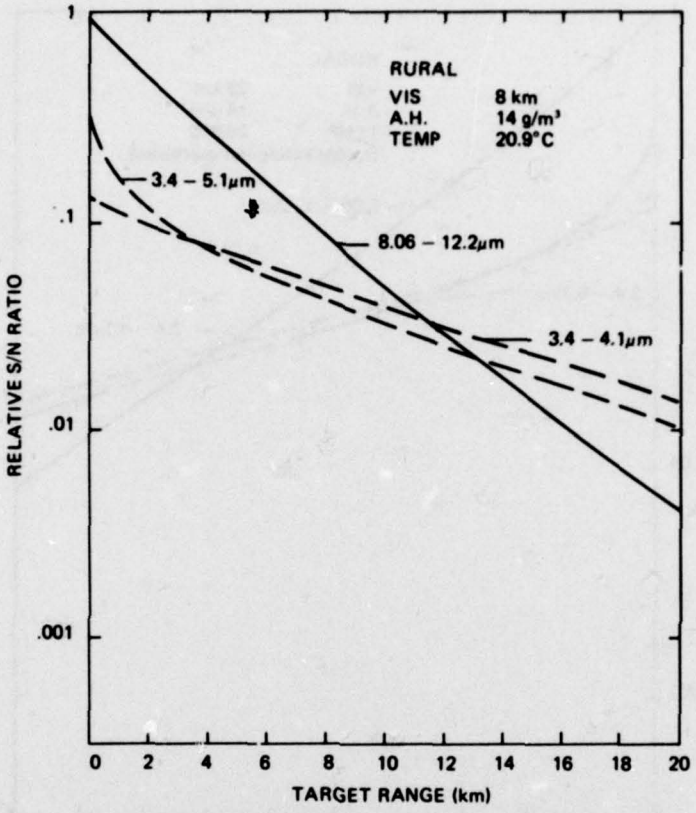

Fig. 9—Relative S/N ratio as a function of range. Note effect of lower visibility compared to Fig. 7. The Rural aerosol model is used.

(assuming no improvement in *MTF*) would, of course, require a higher net transmittance to compensate for the reduced differential photon flux in the 3- to 5-μm region. The corresponding minimum transmittances for equivalent performance with the same ΔT contrast at the target are given in Table 3.

With the above approximations it is then possible to determine the maximum operating range of an advanced-technology system operating in the 3.4- to 4.1-μm band as a function of humidity for a given visibility range. For various visibilities these maximum ranges for targets with $\Delta T \approx 1$K are shown as nearly vertical dashed lines in Fig. 14. With the Rural aerosol model the maximum operating range is 32 km for an advanced 3.4- to 4.1-μm system for a humidity of 14 g/m^3 and a visibility range of 23 km. However, for the same visibility with the Maritime aerosol model this maximum operating range for a target contrast of $\Delta T = 1$K is reduced to 16 km. The imaging of higher contrast targets would increase the maximum operating range. For example, the maximum operating range for a $\Delta T = 4$K contrast target would be 26 km for a Visibility range of 23 km using the Maritime aerosol model. Nevertheless, the introduction of the Maritime aerosol model not only moves the curve of crossover ranges to high humidities, but it also sharply curtails the

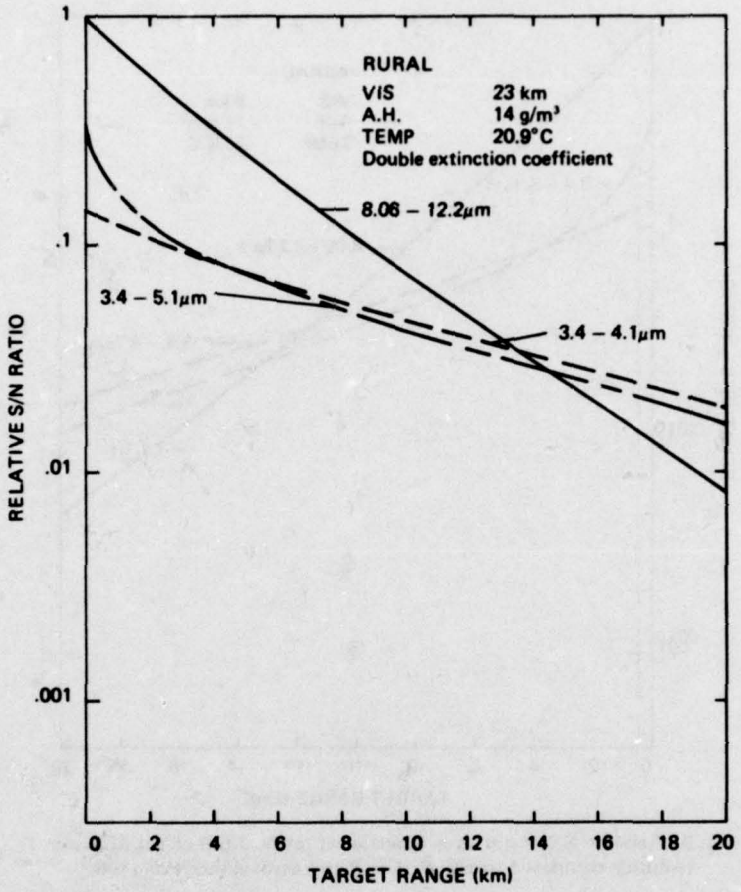

Fig. 10—Relative S/N ratio as a function of range. The 3- to 5-μm water vapor extinction coefficient is twice that used in Fig. 7. The Rural aerosol model is used.

expected maximum operating range of advanced-technology 3- to 5-μm systems. With the Maritime model, even under fairly humid conditions, the region in which an advanced 3- to 5-μm system would have an advantage over the 8- to 12-μm system and could still be expected to accomplish meaningful imaging tasks is restricted. For visibility ranges less than 15 km, this region of advantage in range to the target becomes vanishingly small.

Influence of Optical MTF

For a given optical aperture and diffraction-limited optics, the optical modulation transfer function MTF_{opt} for a 3- to 5-μm system will be superior to that for a 8- to 12-μm system. We have ignored this effect in the comparisons. One approach is to reduce the detector size of the 8- to 12-μm system to try to match the overall *MTFs* of the two systems and then to calculate the effect on $(SNR)_{rel}^{\Delta\lambda}$ of this disparity in detector instantaneous

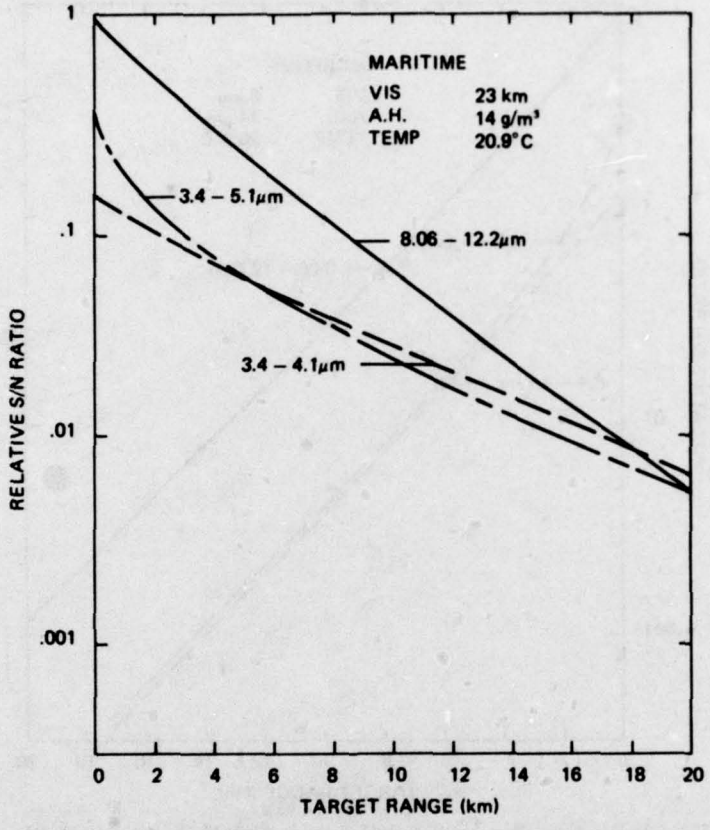

Fig. 11—Relative *SNR* as a function of range. Compare this figure, which uses the Maritime aerosol model, with Fig. 7, which uses the Rural aerosol code.

field of view. Since this approach is not practical for high-resolution systems we will instead keep the instantaneous field of view constant for all wavelengths and include a relative *MTF* factor in $(SNR)_{rel}^{\Delta\lambda}$, such that

$$(SNR)'^{\Delta\lambda} \equiv \frac{MTF_{\lambda opt}}{MTF_{10opt}} SNR_{rel}^{\Delta\lambda} .$$

This factor (MTF_λ/MTF_{10}) is a constant for a given product of resolution element size and aperture diameter and is plotted as a function of this product for $\lambda = 5$ μm in Fig. 15. The influence of the *MTF* factor depends strongly on the angular resolution element size in target space. For example, for an aperture with $D = 25$ cm and a resolution element size of 0.04 mR the 3.4- to 5.1-μm $(SNR)_{rel}^{\Delta\lambda}$ curves should be raised by a factor of 1.8 due to *MTF* effects, whereas for the same aperture and a resolution element size of 0.1 mR the effect is negligible (a factor of 1.2).

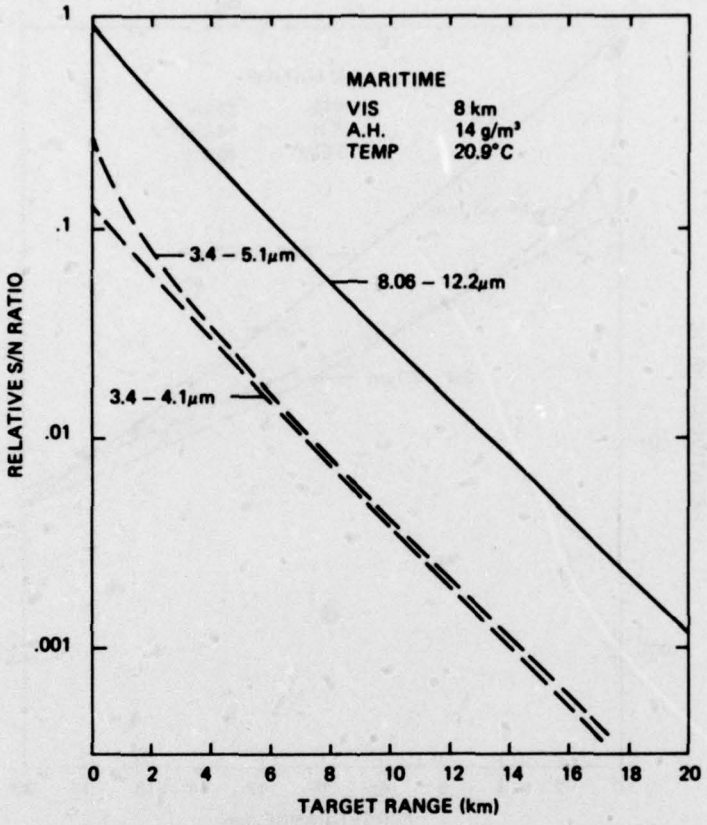

Fig. 12—Relative *SNR* as a function of range. Note the combined effect of Maritime aerosol model and low visibility as compared to Figs. 7 and 11.

In most cases in the infrared the optical *MTF* even from diffraction-limited optics will dominate any image blurring caused by propagation through a turbulent atmosphere. This is, however, not necessarily the case for large optical diameters with 3- to 5-μm systems. Using the approach described in Ref. 11, we estimate that for moderate turbulence ($C_n = 10^{-7}$ m$^{-1/3}$) the long-term *MTF* at $\lambda = 5\mu$m due to atmospheric propagation will compete with the diffraction-limited *MTF* at target ranges longer than 7 km for aperture diameters of 25 cm. (For propagation through 7 km the two *MTFs* have the value of $1/e$ at the same spatial frequency.) The principal effect of including a turbulence *MTF* is to reduce the relative *MTF* advantage of large-aperture 3- to 5-μm systems. Atmospheric turbulence will nevertheless be ignored in our comparisons.

For a specific imaging task with a particular target (for example, classification of a certain size of ship), the angular resolution element size of interest will be a function of range to the target. In that case $(SNR)_{rel}^{\Delta\lambda}$ by itself loses its meaning as a function of range since *MTF* and signal integration factors will be changing along with atmospheric transmission. The ratio of $(SNR)'^{\Delta\lambda}$ to $(SNR)'^{8\text{-}12}$ is still meaningful, however, and will describe the

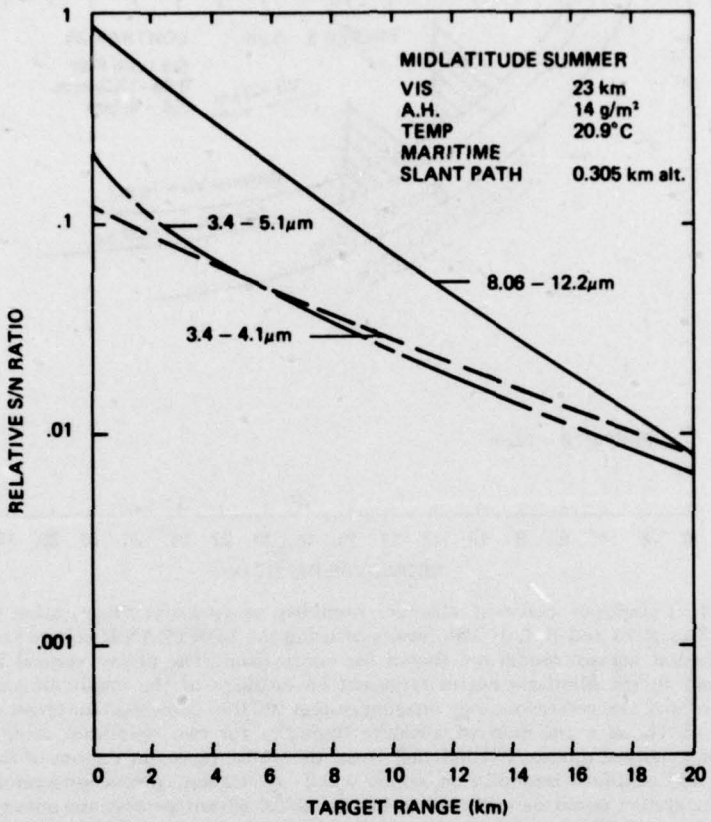

Fig. 13—Relative *SNR* as a function of range, with a slant path from an altitude of 305 m (1000 ft). The Maritime aerosol model is used.

relative advantage of a particular wavelength band at a particular range. Figures 16 through 21 describe $(SNR'^{\Delta\lambda})/(SNR'^{8\text{-}12})$ for a number of atmospheric conditions through a slant path with a maximum altitude of 305 m (1000 ft) and the combinations of target resolution element size optics and aperture diameter listed in Table 4.

At long ranges $(SNR)'^{\Delta\lambda}$ becomes larger for the 3- to 5-μm systems, however, and once again operating range must be estimated to ascertain whether this advantage can be useful. For an advanced-technology 3- to 5.1-μm system we will assume for the performance of meaningful tasks that the minimum value of $SNR'^{\Delta\lambda}$ is 0.005. Regions where $SNR'^{\Delta\lambda}$ is less than this for the 3- to 5.1-μm band are indicated by dashed lines in Figs. 18-21. The influence of *MTF* alone can be estimated by plotting $(SNR'^{\Delta\lambda}/SNR'^{8\text{-}12})$ as a function of range assuming that the atmosphere is 100% transmissive as in Fig. 22.

An overview of the curves leads to several conclusions. Task 1 is dominated by atmospheric transmission. Optical *MTF* effects play a small role to ranges of 30 km. Task 2 is influenced by both *MTF* and atmospheric transmission, and Task 3 is dominated by the

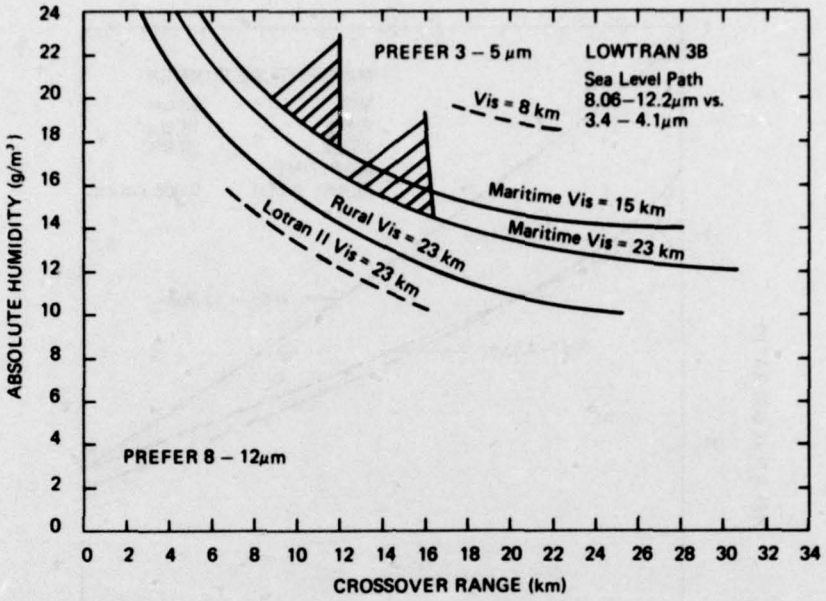

Fig. 14.—Composite curve of absolute humidity vs crossover range, using data from Figs. 6-13 and Ref. 1. The results of using the LOWTRAN II code with the Continental aerosol model are shown for comparison. The nearly vertical lines attached to the Maritime curves represent an estimate of the maximum useful range of an advanced-technology imaging system (20,000 detectors) for target contrasts of 1K as a function of absolute humidity for two visibilities using the Maritime aerosol model. The hatched areas, therefore, represent regions of target range and absolute humidity in which a 3.4- to 4.1-μm, advanced-technology imaging system could be expected to have a useful advantage over the advanced-technology, 8.06- to 12.2-μm system in the presence of a maritime aerosol.

Table 3—Comparison of Bands for Equivalent Performance

Δλ (μm)	Current Technology 200 Detectors— Min. Transmittance	Advanced Technology 20,000 Detectors— Min. Transmittance
8.1 - 12.2	0.1	0.01
3.4 - 5.1	0.292	0.0292
3.4 - 4.1	0.678	0.0678

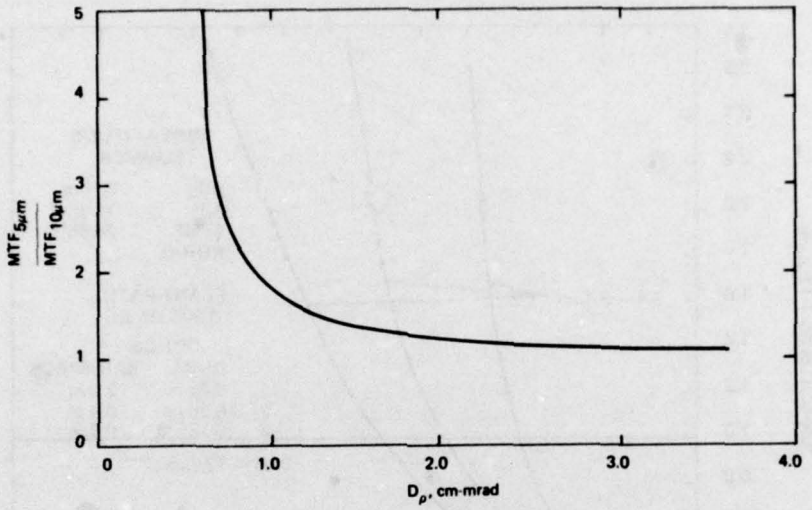

Fig. 15—Plot of the ratio of the diffraction-limited optical modulation transfer function (*MTF*) at $\lambda = 5$ μm to the *MTF* at $\lambda = 10$ μm, as a function of ρD, where ρ is the angular width of the bar in a test pattern and D is the aperture diameter of the refractive optical system.

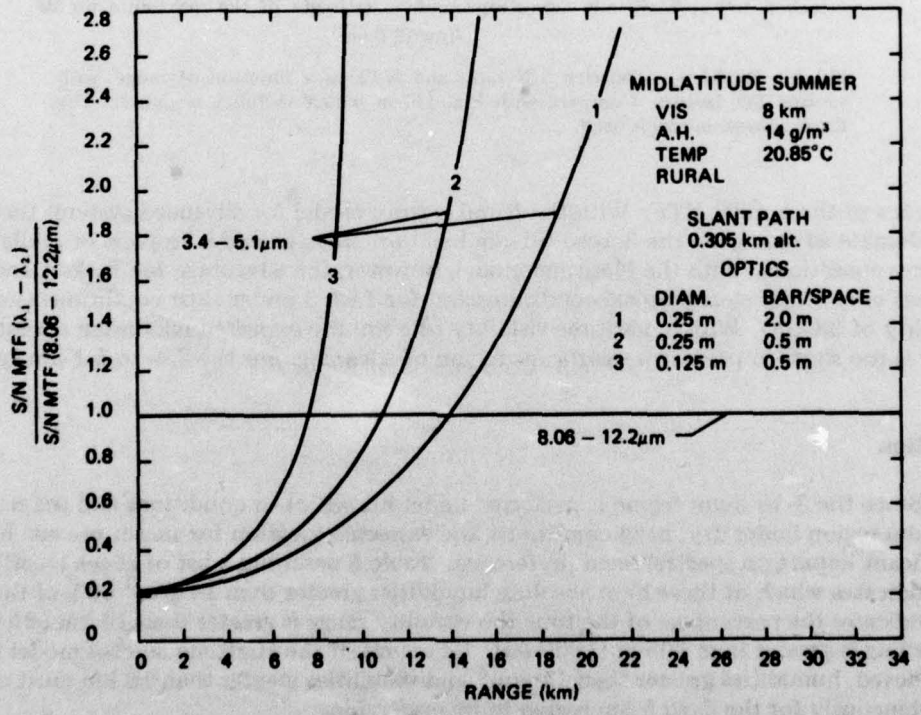

Fig. 16—Products of relative S/N ratio and *MTF* as a function of range, with various $D\rho$ factors. The Rural aerosol model is used.

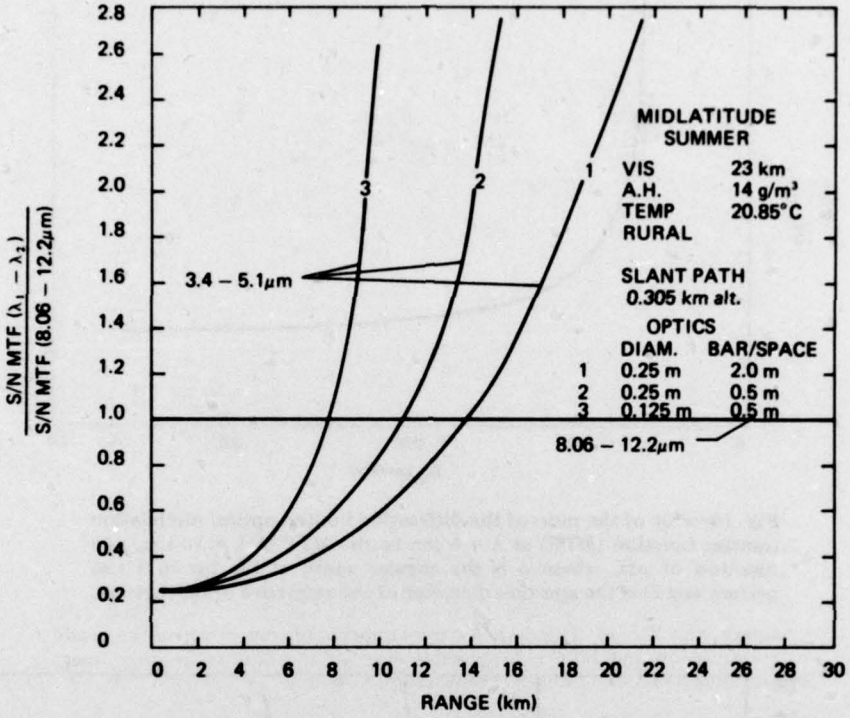

Fig. 17—Products of relative S/N ratio and *MTF* as a function of range, with various $D\rho$ factors. Compare with Fig. 16, in which visibility is poorer. The Rural aerosol model is used.

influence of the optical *MTF*. With the Rural aerosol model for advanced systems there is a considerable advantage in the 3.4- to 5.1-μm band for all tasks under tropical or midlatitude summer conditions. With the Maritime model, however, the advantage for Tasks 1 and 2 remains only under clear tropical conditions and for Task 3 under clear conditions (sea level, visibility of 23 km). With a maritime visibility of 8 km the expected maximum operating range is too short to provide a significant region of advantage for the 3.4- to 5.1-μm system.

Location

Since the 3- to 5-μm region is preferred under humid, clear conditions and the 8.1- to 12.2-μm region under dry, hazy conditions, the expected location for sensor use can have a significant impact on spectral band preference. Table 5 describes a list of at-sea locations and indicates which of these have absolute humidities greater than 14 g/m^3 60% of the time and indicates the percentage of the time the visibility range is greater than 16 km (whenever the ceiling is greater than 305 m (1000 ft)). Of course, if the Maritime aerosol model is to be believed, humidities greater than 14 g/m^3 and visibilities greater than 16 km must occur simultaneously for the 3- to 5-μm region to be preferable.

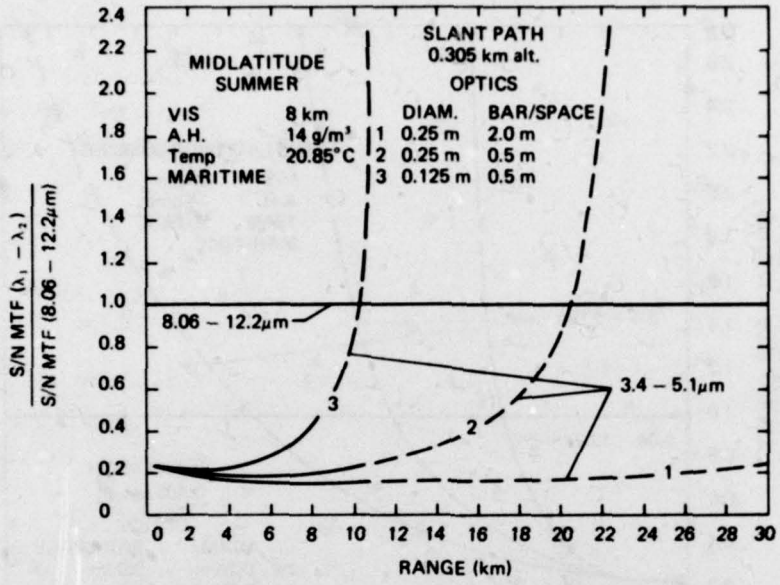

Fig. 18—The effect of changing from the Rural to the Maritime aerosol model. Compare with Fig. 16. The dashed curves indicate regions in which the product of transmission and *MTF* is low, where even an advanced-technology imaging system may be unable to perform meaningful tasks.

THE MARITIME AEROSOL MODEL

The analysis presented so far demonstrates that the maritime character of the aerosol can have a profound influence on spectral band preference. The maritime particle size density distribution incorporated into LOWTRAN 3B by Shettle and Fenn [13] is shown in Fig. 23. The distribution is supposed to correspond to a relative humidity of 80% and moderate windspeeds. Although it is acknowledged that the size distribution will in actuality be a function of windspeed, relative humidity, and altitude, in the LOWTRAN 3B code only the total particle number density is varied both as a function of sea level visibility range and altitude. The same particle size distribution is used for all calculations. Thus, the ratio of the extinction due to aerosol at a particular IR wavelength to the extinction in the visible remains constant as visibility range and altitude change (for altitudes under 2 km). The increased extinction in the 3- to 5-μm region with the Maritime model is caused by the sea spray-induced bulge in the particle size distributions around a particle radius of 2 μm. In reality this spray-induced component could be a strong function of altitude, so that the extinction in the 3- to 5-μm region could be lower for slant paths than is currently predicted by LOWTRAN.

Figure 24 plots extinction due to the various LOWTRAN aerosol distributions as a function of wavelength normalized to a visibility range of 23 km. Clearly the relationship between extinction in the visible, which can be characterized by a visibility range, and extinction in the 3- to 5-μm region due to aerosols is drastically altered by the introduction of the Maritime model distribution. The extinction near 10 μm is dominated by absorption

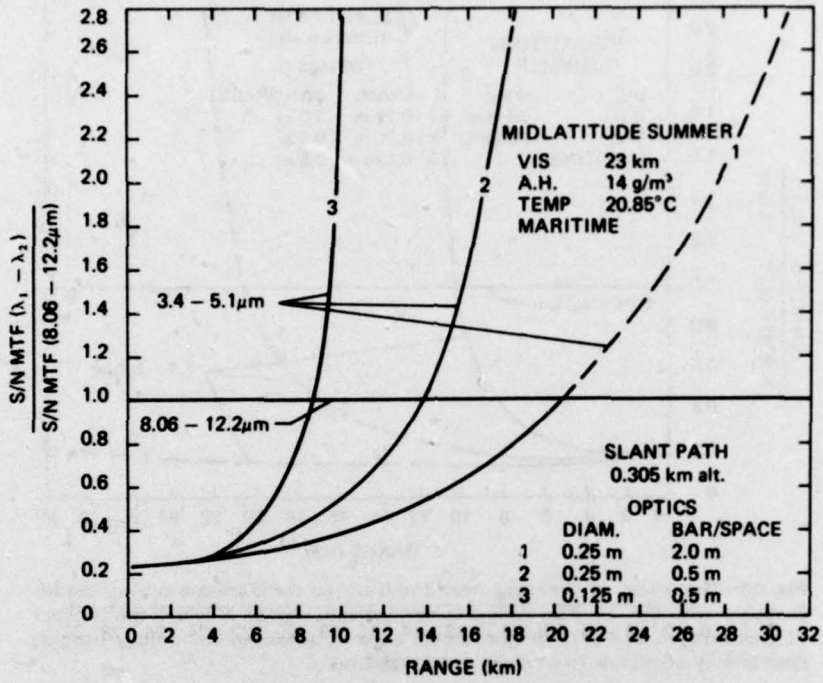

Fig. 19—Products of relative *SNR* and *MTF* as a function of range. A dashed curve is used to identify regions where the product of transmission and *MTF* is low. The Maritime aerosol model is used.

in the droplets rather than scattering, whereas, in the 3- to 5-μm region scattering is also important. If decreased visibility were caused by a growth in particle size rather than by an increase in number it is likely that the ratio of the aerosol extinction coefficient in the two wavelength regions would change as visibility decreased.

Experimental data for a maritime environment are rare, and even comparisons with other transmission codes are difficult since the other codes often use different input variables (i.e., windspeed and relative humidity instead of visibility range). However, Table 6 summarizes currently available information concerning extinction coefficients. Representative values from several runs are used.

The EMI data were taken with a low-level, over-water path. Winter extinction measurements are summarized in the EMI Table 6 entry under the assumption that those are aerosol dominated.

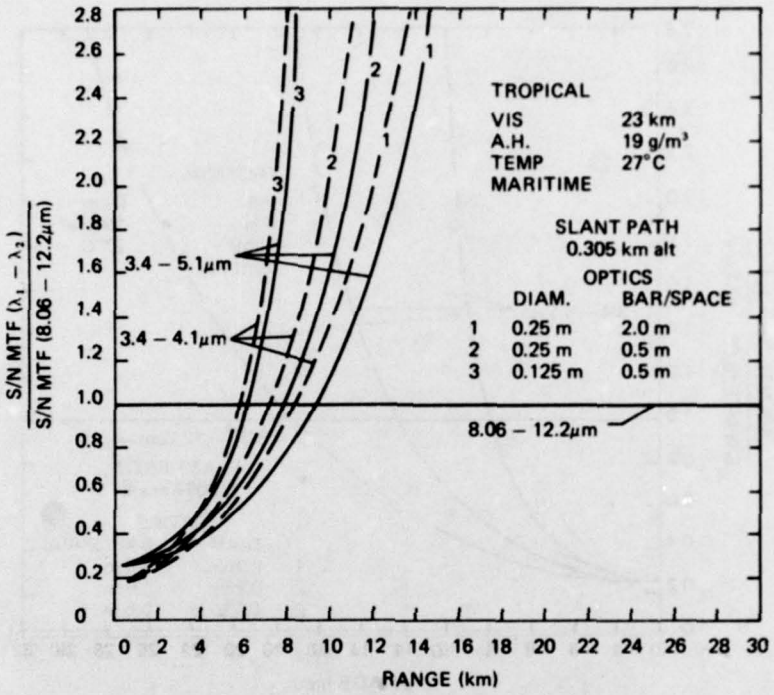

Fig. 20—Products of relative *SNR* and *MTF* as a function of range. The Maritime aerosol model is used.

CONCLUSIONS

With comparable quality detectors, present-technology thermal imaging systems (≈200 detectors) should provide superior performance if they are designed to operate in the 8- to 12-μm spectral band. With an advanced technolgy (≈20,000 detectors), operation in the 3- to 5-μm band will be preferred from a *SNR* point under humid conditions or whenever optical *MTF* effects dominate if the Rural aerosol model is appropriate.

The introduction of the Maritime aerosol model, however, strongly affects the *SNR* ratio tradeoff since for a given visibility range, 3- to 5-μm transmission is reduced. Under moderate visibility condition (8 km) the 8- to 12-μm region seems to be preferred even under fairly humid conditions. With the Maritime aerosol model, the advantage of the 3- to 5-μm band as to atmosphere transmission is restricted to clean visibility of (23 km) humid conditions. In many cases with the Maritime aerosol distribution, even an advanced technology 3- to 5-μm system will be unable to perform meaningful tasks at ranges long enough to experience *MTF* and atmospheric transmission advantages.

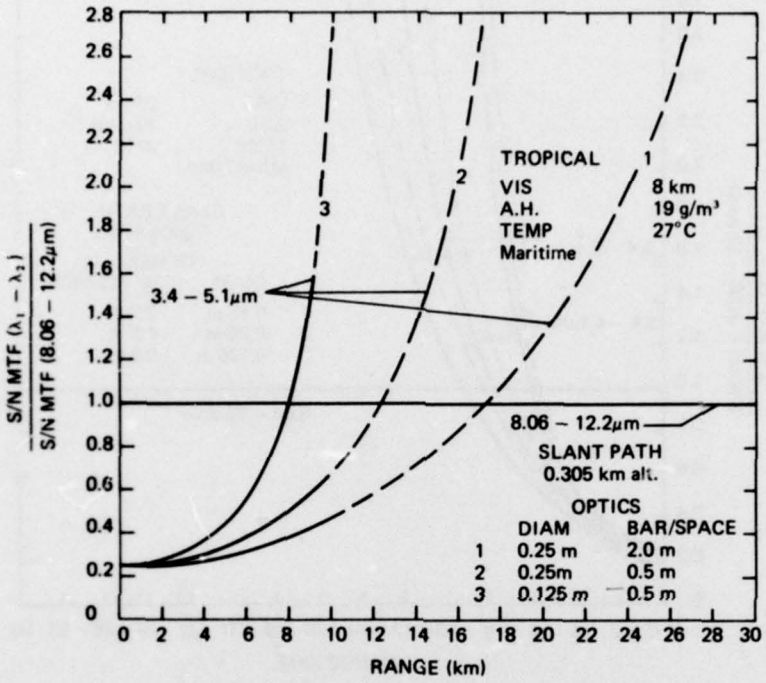

Fig. 21—Products of relative *SNR* and *MTF* as a function of range. Dashed lines indicate regions where the product of transmission and *MTF* is low.

Table 4—Aperture Sizes Required for Various Tasks

Task No.	Target Resolution Element Size* (m)	Optics Aperture Diameter (cm)	Classification Task
1	2	25	Large ship as viewed from a patrol aircraft
2	0.5	25	Small boat as viewed from a patrol aircraft
3	0.5	12.5	Tank as viewed from and attack aircraft

*Width of the bar in a bar chart.

Recommendations

Experimental verification of the IR extinction to be expected with maritime aerosols is needed before intelligent focal plane array technology development choices use at sea can be made. Particular attention should be given to transmission in the 3- to 5-μm band for slant paths that would be characteristic of air-to-ground surveillance.

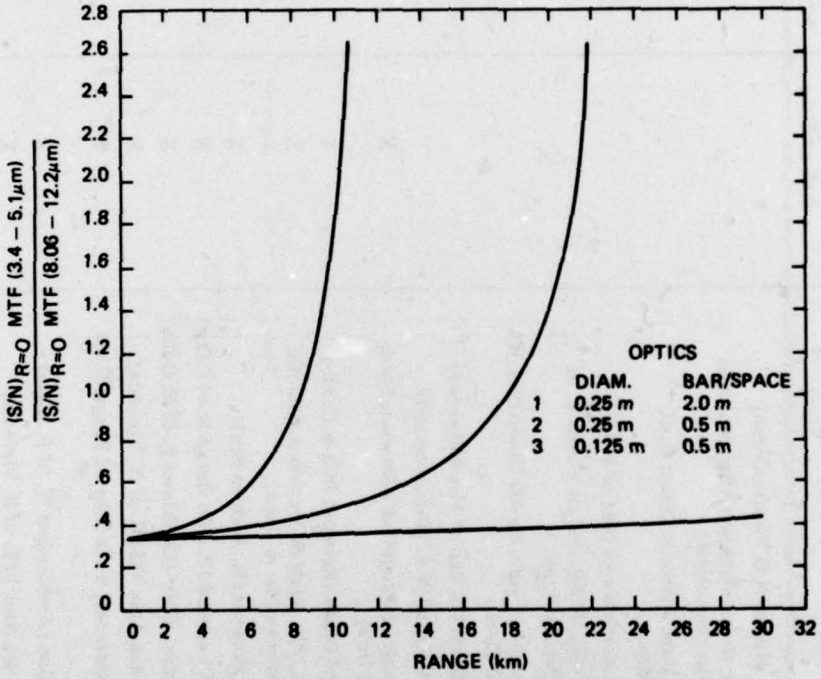

Fig. 22—Effect of *MTF* on the product of *SNR* and *MTF*, assuming no atmospheric extinction.

Table 5—Absolute Humidities and Ceiling for Various Parts of the World*

Latitude	Longitude	Site Description	Water Vapor > 14 g/m^{-3} 60% of Time	Water Vapor < 14 g/m^{-3} 60% of Time	Vis > 16 km, Ceiling $> 1000'$ (%)
56 N.-Coast	151-157 W.	Kodiak, Alaska (N.E. Pacific Ocean)		X	
45-47 N.	53-56 W.	Argentia, Newfoundland (Atlantic Ocean S.E. of Newfoundland)		X	54
42 N.-Coast	66 W.-Coast	Boston, Mass. (Atlantic Ocean E. of central Mass.)		X	69
39.7 N.	129.4 E.	Wonsan, North Korea (Sea of Japan)		X	
38-40 N.	72 W.-Coast	Atlantic City, N.J. (Atlantic Ocean E. of S. N.J., Del., & N. Md.)		X	76
36-38 N.	126 W.-Coast	San Francisco, Calif. (Pacific Ocean S. & W. of central Calif.)		X	72
63.0 N.	3.4 W.	Malaga, Spain (W. end of Mediterranean)			92
32.2 N.	33.3 E.	Port Said, Egypt (S.E. Mediterranean)			95
27.2 N.	50.2 E.	Northwestern Persian Gulf (Between Saudi Arabia & Iran)	X		
25.0 N.	57.8 E.	N. Gulf of Oman (Between Iran & Oman)	X		
23-25 N.	79-83 W.	Key West, Fla. (Gulf of Mexico & Atlantic Ocean between Fla. & Cuba)	X		91
29.9 N.	67.8 E.	Karachi, Pakistan (N. Arabian Sea)	X		
20.4 N.	158.3 W.	Hawaiian Leeward (Pacific Ocean S. of Oahu)	X		
18-20 N.	74-76 W.	Guantanamo, Cuba (Caribbean S. of E. Cuba)	X		95
17-22 N.	110 E.-Coast	S. China Sea Area VII (E. of N. Vietnam)	X		
17.9 N.	85.2 E.	Vishakhapatnam, India (Bay of Bengal E. of S. India)	X		
14.2 N.	73.0 E.	Panjim, Goa (Arabian Sea W. of S. India)	X		
11-14 N.	111 E.-Coast	S. China Sea Area I (E. of S. Vietnam)	X		
7-11 N.	102 & 103 E-Coast	S. China Sea Area VI (Gulf of Siam adjoining Malaysia)	X		

*From Ref. 10.

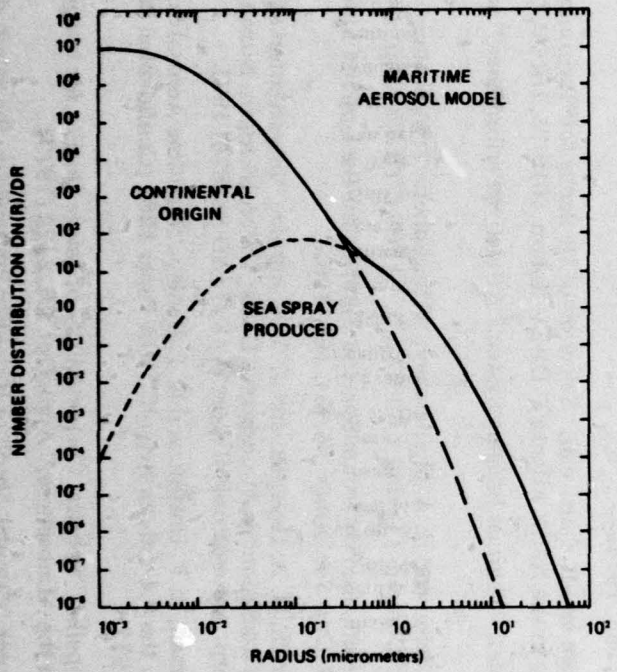

Fig. 23—Plot of particle-size distribution in the Maritime aerosol model used in LOWTRAN 3B.

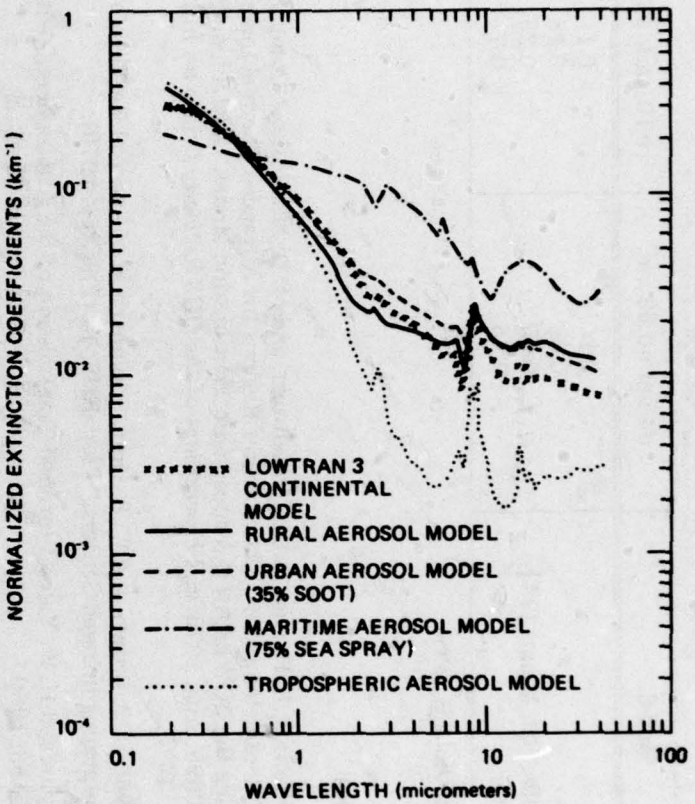

Fig. 24—Variation in extinction coefficient with wavelength for the various aerosol distributions used in LOWTRAN 3B. The curves are all scaled to a visibility range of 23 km.

Table 6—Aerosol Model Extinction Coefficients*

Model	$\sigma 4\ \mu m/\sigma 0.53\ \mu m$	$\sigma 10\ \mu m/\sigma 0.53\ \mu m$
Rural	0.1	0.1
Maritime	0.6	0.18
Katz (Wells, Gal, Munn) [14]	0.65	0.23
EMI (Data)	0.75	0.7

*Comparison of Visibility 23 km.

REFERENCES

1. A. F. Milton, G. L. Harvey, J. C. Kershenstein, and M. D. Mikolosko, "Comparison of the 3-5 Micrometer and 8-12 Micrometer Regions for Advanced Thermal Imaging Systems Using the LOWTRAN 2 Atmospheric Transmission Model," NRL Memorandum Report 3098, Aug. 1975; and *Proceedings of the IRIS Specialty Group on Infrared Imaging*, 1975.
2. H. Barhydt, D. P. Brown, and W. B. Dorr, "Comparison of Spectral Regions for Thermal-Imaging Infrared Sensors," Proc. IRIS, 14 (2), (Aug. 1970).
3. J. H. Taylor and H. W. Yates, "Infrared Transmission of the Atmosphere," NRL Report 5453, 1960.
4. A. D. Schnitzler, "The Composite FLIR-Visual System I: Quantitative Relationships Between Performance and Design Parameters," The IRIS Imaging Specialty Group Meeting, Jan. 1974.
5. W. G. Tam and R. Corriveau, "Selection of IR Bands for Horizontal Detection and Tracking in the North Atlantic," DREV Report 4010/75, DREV, Courcelette, Que.
6. T. W. Tuer, "Thermal Imaging Systems, "Relative Performance," submitted to Applied Optics.
7. J. E. A. Selby and R. A. McClatchey, "Atmospheric Transmittance from 0.25 to 28.5 Microns: Computer Code LOWTRAN 3," AFCRL-TR-75-0255.
8. W. A. Kleinhans, "Optimum Spectral Filtering for Background Limited Infrared Systems," *J. Opt. Soc. Amer.* 55, (1), 104 (1965).
9. D. E. Burch, D. A. Gryvnak, and J. D. Pembroke, "Investigation of the Absorption of Infrared Radiation by Atmospheric Gases: Water, Nitrogen, Nitrous Oxide," Philco Ford Corp. Aeronutronic Report U-4897 (AD 882876) 1971.
10. A. Guttman, R. F. Horton, and S. T. Hanley, "Maritime Aerosol Scattering Measurements in the 0.4-4.0-μm Region," IDA Paper 1281 (Confidential Paper, Unclassified Title), 1977.
11. N. S. Kopeika, "Spectral Characteristics of Image Quality for Imaging Horizontally Through the Atmosphere," Appl. Opt. 16, 2422 (1977).
12. P. M. Moser, "Annual Absolute Humidity Probabilities for Selected Marine Locations," Technical Memorandum NAD-20203: PMM, Feb. 24, 1973.

13. E. P. Shettle and R. W. Fenn, "Models of the Atmospheric Aerosols and Their Optical Properties," AFCRL, Hanscom AFB.

14. W. C. Wells, G. Gal, and M. W. Munn, "Aerosol Distributions in Maritime Air and Predicted Scattering Coefficients in the Infrared," *Appl. Opt.* 16, (3), 654 (Mar. 1977).

Appendix A

WATER VAPOR CONTINUUM FOR 3 TO 5-μm

When attenuation occurs over a broad band and is apparently not caused by well-defined absorption lines, the attenuation is attributed to continuum absorption. In the 3- to 5-μm region it is thought that attenuation due to water vapor continuum absorption exists, but there is not enough measured data on which to base a model. It has been suggested that the values of 3- to 5-μm water vapor continuum absorption used in LOWTRAN 3B should be from zero to several times the values contained in the model.

The equation for calculating transmission at a particular wavelength in LOWTRAN 3B has the form

$$t = (e^{-AR})e^{-C_\nu kR}$$

where t is the transmission, A is the attenuation coefficient for molecular absorption, C_ν is a coefficient for the 3-5 μm water vapor continuum absorption associated with the wavelength, the constant k is a function of the percipitable water, the pressure, and the temperature and R is the range. The exact form of the equation for transmission is complicated by several correction factors and is given below in the complete form in which it occurs in LOWTRAN 3B: The extinction coefficients associated with other gases are included in the factor A.

$$t = (e^{-AR})e^{-R(0.1\ WH)\ [PPW\ +\ 0.12\ (PS\ -\ PPW)]e^{4.94/TS}\ (1.05\ \times\ 10^{-3})C_\nu}$$

where WH is the water vapor density, PPW is the partial pressure of water vapor, PS is the total pressure in atmospheres, and TS is the ratio 273.0 K over the air temperature in degrees Kelvin.

There are 15 values of C_ν between the frequencies 2350 and 300 cm^{-1} (3.3-4.25 μm) given at the intervals of 50/cm in the LOWTRAN 3B code. The maximum value of C_ν is 0.330 at 3000 cm^{-1}, and the minimum is 0.087 at 2600 cm^{-1}. For this analysis the program was modified so that C_ν could be multiplied by any desired value. All runs but one were made using the values of C_ν contained in the program. For the plot shown in Fig. 10 the values of C_ν were multiplied by two.

Appendix B

MAXIMUM RANGE ESTIMATES

The estimates given in Table B1 for the minimum useful atmospheric transmittance for an advanced-technology, 20,000-detector imaging system, of course, depend on the imaging task being performed and on the other parameters of the particular imaging system.

These estimates were obtained by analyzing the expected performance of imagers with entrance apertures of 25 cm and 20,000 BLIP detectors. Each imager used a different spectral passband. A magnification of 20, an overall field of view of $1.9^\circ \times 2.5^\circ$, a 40-$\mu R$ detector instantaneous field of view, a photodiode detector quantum efficiency of 0.5, and an *MTF* limited solely by the diffraction-limited refractive optics and the detector size were assumed in all three cases.

Minimum resoluable temperature difference as a function of spatial frequency curves were derived scaling from the results of A. D. Schnitzler to be published in an IDA paper "Effects of Focal Plan Arrays, *MTF* and Atmospheric Attenuation on the Predicted Performance of FLIR Imaging Systems." In the low-spatial-frequency regime the *MRT* curves are flat as a function of spatial frequency. These curves show that with atmospheric transmission to the target greater than those shown in Table B1 there will be a greater than 50% probability of detection for bar chart targets with a bar: to-space temperature difference ΔT of 1 K and spatial frequencies less than approximately 4 cycles per milliradian for the 8- to 12.2-μm system and less than 8 cycles per milliradian for the 3- to 5-μm system. A bar pattern target with four bars and a length-to-width ratio of 7 to 1 was assumed in all cases. In practice, at low spatial frequencies with focal plane arrays the *MRT* may be limited by spurious effects associated with pattern noise in the background arising from the intervening atmosphere. This is hard to quantify and is ignored in the estimate presented here.

For $\Delta T = 1K$ bars of width 2m the minimum transmission estimates in Table B1 are therefore reasonable to target ranges of 16 km for the 8.1- to 12.2-μm system and 32 km for the 3- to 5-μm systems. At longer ranges with 2-m bar pattern targets with $\Delta T = 1$ K, higher total transmittance will be required due to *MTF* and signal integration effects. Smaller targets will require even higher transmittance as the range increases.

Table B1—Comparison of Bands for Equipment Performance

$\Delta\lambda$ (μm)	Current Technology 200 Detectors— *Min. Transmittance*	Advanced Technology 20,000 Detectors— *Min. Transmittance*
8.1 - 12.2	0.1	0.01
3.4 - 5.1	0.292	0.0292
3.4 - 4.1	0.678	0.0678